MODELING SEASONALITY IN AVIAN INFLUENZA H5N1

NECIBE TUNCER AND MAIA MARTCHEVA*

Abstract. The number of cases of avian influenza in birds and humans exhibits seasonality which peaks during the winter months. What causes the seasonality in H5N1 cases is still being investigated. This article addresses the question of modeling the periodicity in cumulative number of human cases of H5N1. Three potential drivers of influenza seasonality are investigated: (1) seasonality in bird-to-bird transmission; (2) seasonality caused by wild bird migration or seasonal fluctuation of avian influenza in wild birds; (3) seasonality caused by environmental transmission. A framework of seven models is composed. The seven models involve these three mechanisms and combinations of the mechanisms. Each of the models in the framework is fitted to the cumulative number of humans cases of H5N1. The corrected Akaike Information Criterion (AICc) is used to compare the models and it is found that the model with periodic bird-to-bird transmission rate best explains the data. The best fitted model with the best fitted parameters gives a reproduction number of highly pathogenic avian influenza $\mathcal{R}_0 = 1.06$. The best fitted model is a simple SI epidemic model with periodic transmission rate and disease-induced mortality, however, this model is capable of very complex dynamical behavior such as period doubling and chaos.
Keywords: mathematical models, non-autonomous differential equations, reproduction number, seasonality, H5N1, avian influenza, model selection.

AMS Subject Classification: 92D30, 92D40

1. Introduction

Fifteen years after its appearance leading to the death of a boy in Hong Kong, in 1997, the highly pathogenic avian influenza (HPAI) of subtype H5N1 continues to infect humans and cause nearly 60% death rate among the affected individuals [23]. Despite the low count of infected humans, 637 as of October 2013, the HPAI H5N1 is considered one of the most dangerous diseases that humanity faces today[52]. The fear stems from the possibility that the now zoonotic microorganism may emerge at some point as an efficiently human-to-human transmissible pathogen, capable of killing millions of people in a short period of time [14].

The virus circulates primarily in poultry and has proven a formidable opponent to the control measures. Millions of chickens have been destroyed in an attempt to eliminate the pathogen. Early reports in many countries in Asia proclaimed the virus "stamped out", only for the culprit to return a few months later during the cooler time of the year [32].

Now it is well known that the dynamics of H5N1 infections in both domestic birds and humans follows seasonal pattern with peaks during December-April, and lows during June-September periods, much like human influenza in the temperate climates in the Northern Hemisphere (see Figure 1, [11], and [31]). The pattern can be seen across all

Date: October 4, 2013.
*author for correspondence.

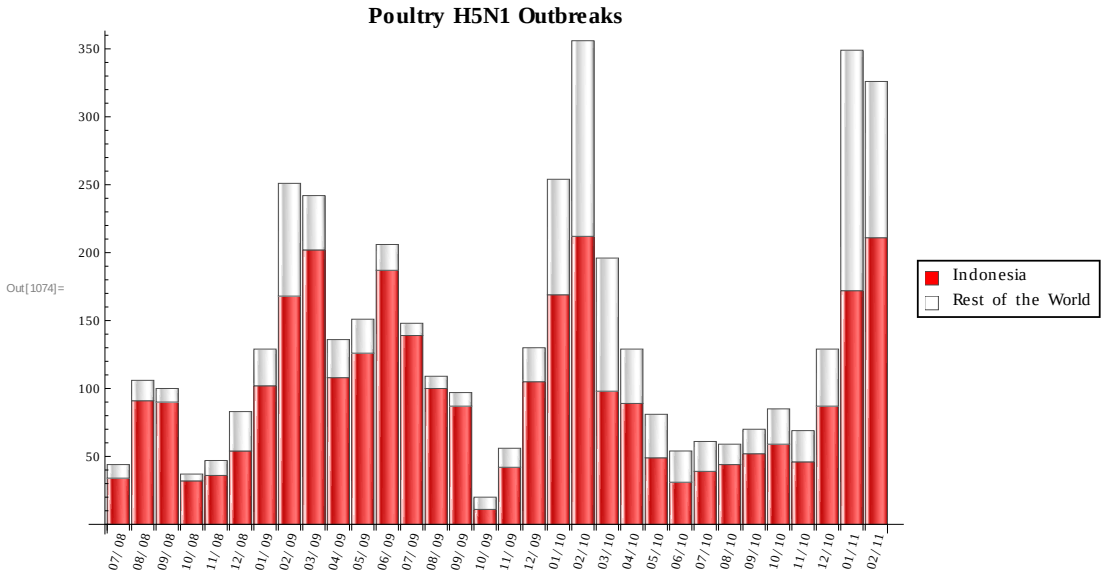

FIGURE 1. A bar chart of monthly poultry outbreaks in the period 2008-2011. Red portion of the bar represents poultry outbreaks in Indonesia, and white portion – poultry outbreaks in the rest of the world. The main contributor in the remainder of the world is Egypt.

affected countries, most of which are in fact tropical countries with warmer weather. To show the seasonality in the poultry outbreaks, we produced the Figure 1, from the monthly FAO reports [11]. The tallest bar in the bar chart (see Figure 1) occurs on February 2010. In February 2010, total of 7 countries (including Indonesia) reported FAO a total of 356 poultry outbreaks of which 212 occurred in Indonesia and the rest in countries such as Egypt and Viet Nam (see Figure 1 in the February 2010 report in [11]). In Figure 1, we plotted the Indonesia outbreaks in red, and the rest of the world in white. This is the way other bars are produced in the bar chart. Table 1 gives the number of outbreaks for the period 2008 to 2011 used to produce the bar chart. A poultry outbreak means the detection of one H5N1 infected domestic bird in a farm. For instance, two outbreaks in a village means there are two farms in that village where H5N1 is observed, but the number of birds effected by the virus is not known.

The question of what drives the seasonality in avian influenza is just beginning to be addressed [27] but it has been widely studied for human influenza. Human influenza A also exhibits pronounced seasonality which in temperate zones peaks during the colder winter months. Reasons for the influenza's distinct seasonality in moderate climates are not completely understood. Lofgren *et al.* [22] reviews a number of mechanisms that could be responsible for the observed dynamics. Low humidity and cold temperatures are most often pointed to be reasons for the spike of influenza activity in winter months [34]. Those conditions favor the aerosol-borne influenza virus, which survives longer even on surfaces under colder temperature. Similar correlation between environmental survival of the pathogen and temperature/humidity has been also established for HPAI H5N1 [46]. For human influenza, it is furthermore suspected that low winter temperatures promote crowding among the human population which facilitates transmission. In addition, seasonal variations in the host immune system may play a role. For instance,

TABLE 1. Poultry Outbreaks From 2008-2011

Date	Indonesia	Rest of the World	Date	Indonesia	Rest of the World
07/08	34	10	11/09	42	14
08/08	91	15	12/09	105	25
09/08	90	10	01/10	169	85
10/08	32	5	02/10	212	144
11/08	36	11	03/10	98	98
12/08	54	29	04/10	89	40
01/09	102	27	05/10	49	32
02/09	168	83	06/10	31	23
03/09	202	40	07/10	39	22
04/09	108	28	08/10	44	15
05/09	126	25	09/10	52	18
06/09	187	19	10/10	59	26
07/09	139	9	11/10	46	23
08/09	100	9	12/10	87	42
09/09	87	10	01/11	172	177
10/09	11	9	02/11	211	115

vitamin D levels affect immunity by supporting CD4 T-cell and mucosal antibody responses but vitamin D levels are related to solar or artificial UV radiation and fluctuate seasonally. It is possible that several mechanisms work synchronously to produce the seasonal variations in influenza dynamics.

In contrast, in tropical climates human influenza exhibits fluctuation but the pattern is harder to recognize and appears to be region-specific. Some regions observe outbreaks that follow rainfall season while others see several peaks but no particular association with rainfall [15].

The mechanisms that drive the seasonality of HP H5N1 influenza may be similar to those that drive seasonality in human influenza, or may be specific to the birds who are the main host of avian influenza. Seasonality is typical not only for HP H5N1 influenza in birds but also occurs for low pathogenic strains (LPAI) that infect wild birds [47]. However, the pattern of seasonality in LPAI may be different. Most species of wild birds are infected only some seasons. For instance, shorebirds are infected during spring and fall, while marine birds are frequently infected during summer and rarely infected during spring. The only group of wild birds that carries avian influenza viruses year-round is waterfowl. Avian influenza exhibits distinct seasonality in waterfowl with a peak in late summer when the numbers of highly susceptible juveniles is high. The prevalence of avian influenza decreases in the fall and winter, and it is lowest in the spring when the prevalence reaches a low of 0.25% ([47], Chapter 22).

In this article we address the question of modeling the seasonality of H5N1. Seasonality in avian influenza transmission has been rarely modeled. Most models of HPAI H5N1 created up to date are autonomous and average out the seasonality (but see [23]). Breban *et al.* [4] model seasonality and environmental transmission of low pathogenic avian influenza (LPAI) viruses in wild birds with the basic premise that seasonality is introduced by the migratory patterns and seasonal breeding. The various possible drivers of H5N1 seasonality have not been explored. We do that here and we search for the modeling approach that best accounts for the number of cumulative human cases of H5N1 as given by the World Health Organization [52]. In the next section we discuss

the possible role of climatic factors in the seasonality of avian influenza H5N1 in birds and humans. In section 3, we introduce the basic assumed drivers of seasonality and incorporate them in the simplest way into the H5N1 models. In section 4 we introduce the modeling framework which consists of seven models and we pre-estimate some of the parameters. In section 5 we describe our fitting procedure, and the results of the fitting. Fitting is used to compare each of the seven models to the data. In section 6 we discuss some of the mathematical properties of the best fitted model. Section 7 contains the discussion of the results.

2. Avian influenza seasonality and climate

Can climatic variables such as temperature, rainfall, or relative humidity be associated with H5N1 outbreaks and serve as predictors of seasonality? Association between temperature and poultry outbreaks has been previously found in China [21] where outbreaks occur when temperature is low. Furthermore, Fang et al. [8] found that each 100 mm increase in total annual precipitation is correlated to a 0.9-fold reduction in odds of H5N1 poultry outbreaks in China. However, concluding that outbreaks are correlated with climate on global scale will be premature. A recent article focuses on the seasonality of HP H5N1 in Egypt and Indonesia – two of the most affected countries by poultry outbreaks and human cases [27]. The authors find that human incidence in Egypt is correlated with meteorological factors while this association in Indonesia does not exist. Furthermore, Figure 2 suggests that association between low temperatures and outbreaks high intensity also holds for Egypt but does not hold for Indonesia where temperature remains constant throughout the year. Association between the outbreaks and the rainfall is also hard to establish on a global scale. In Indonesia and Egypt peak of outbreaks coincides with the rainy season, while in Vietnam peak of outbreaks coincides with the dry season and the rainfall season is in the summer months when there are fewer outbreaks (see Figure 2). Thus, climatic factors cannot be easily implicated in the seasonality of H5N1, particularly on a global scale.

We found even less correlation between average humidity and poultry outbreaks (results not shown). This diversity of the climatic characteristics across countries prevents the inclusion of seasonally forced climatic factor (such as temperature or rainfall) as driver of seasonality in H5N1 models. The relationship, if one exists, between climate and H5N1 seasonality is more subtle and may be best accounted for indirectly.

3. Modeling H5N1 seasonality: basic mechanisms

In the absence of a clear understanding of what drives the seasonality in H5N1 influenza, in this section we propose three hypothetical mechanisms that may be responsible for the seasonality of H5N1 influenza in poultry. We propose a simple SI nonautonomous epidemic model to incorporate each scenario. These mechanisms are: (1) seasonality in the transmissibility of H5N1, possibly due to climatic reasons; (2) seasonality introduced by the migration of wild birds or by seasonality in H5N1 cases in wild birds; (3) seasonality in the environmental transmission of the pathogen.

3.1. **Seasonality in the direct transmissibility of H5N1 among poultry.**

The only climatic variable that seems to be associated with outbreaks in all three countries that we investigated (Egypt, Indonesia and Vietnam) is the average number of hours

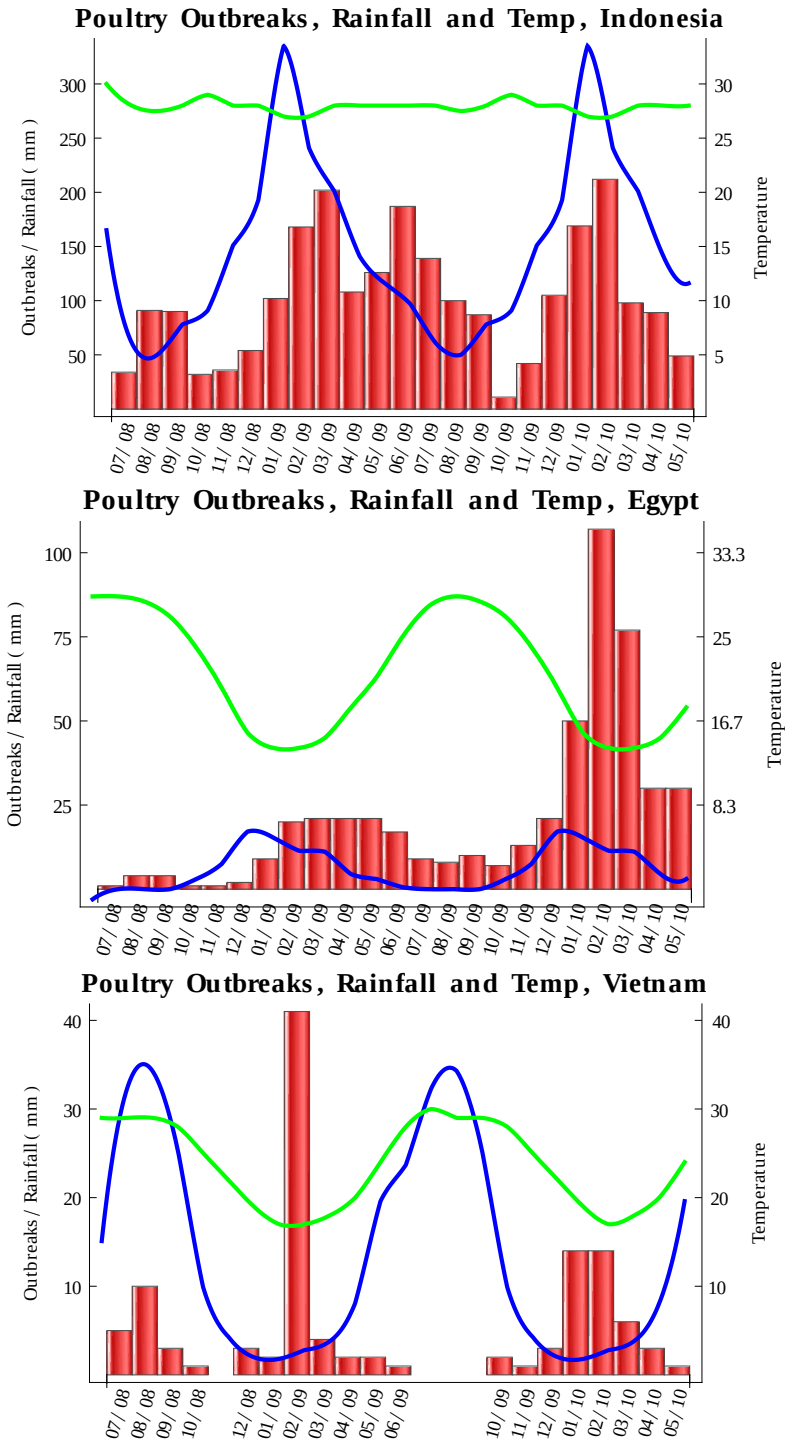

FIGURE 2. A bar chart of monthly poultry outbreaks in the period 2008-2010, rainfall and temperature for Indonesia, Egypt and Vietnam. Poultry outbreaks exhibit seasonality with peak in winter months in all three countries. At the same time temperature is nearly constant in Indonesia. Rainfall is synchronized with the outbreaks in Indonesia where peak rainfall coincides with peak of outbreaks but in Vietnam peak outbreaks coincide with the dry season. Red bars give the outbreaks, blue bars – the rainfall, and the green line is the temperature.

TABLE 2. Definition of the variables in the modeling framework

Variable	Meaning
S_d	Susceptible domestic birds
I_{H_d}	Birds infected with HPAI
V	Amount of virus in the environment
S	Susceptible humans
I	Infected humans with HPAI

of sunlight per day. The average number of hours of sunlight per day is highest in the summer months May-September, and lowest in the winter months. Sunlight and UV radiation in humans affect vitamin-D and melatonin levels which in turn have effect on host susceptibility to influenza [13]. This may suggest that similar mechanisms play role in poultry and affect the seasonality of H5N1 in both poultry and humans. We model this type of seasonality as seasonally forced susceptibility in the direct bird-to-bird transmission of H5N1.

Birds infected with HPAI shed more through the respiratory tract which is in contrast to LPAI where transmission is primarily through the fecal-oral route. Preferential shedding through the oropharynx has been consistently shown with HP H5N1 viruses [9], meaning that direct bird-to-bird transmission of the virus is the primary route of transmission for HP H5N1. The period of survival of the virus in bird secretions, feces, and as aerosols depends on a number of factors, including ambient temperature and humidity which fluctuate with seasons [49] and may contribute to H5N1 seasonality. This type of seasonality again can be modeled as seasonally forced transmissibility in the direct bird-to-bird transmission of H5N1.

To introduce the first model, we divide the domestic bird population into 2 classes: susceptible birds, S_d and infected birds with HPAI, I_{H_d}. We use a simple SI model for the dynamics of HPAI among poultry, since almost all birds infected with avian influenza either die from infection or are culled to prevent the spread of the disease. The model for the bird population is coupled with a simple SI model for the human population that captures the zoonotic transmission of H5N1 to humans. The dynamic variables of the human portion of the model are S – the number of susceptible humans and I – the number of infected humans. The description of the dynamic variables can be found in table Table 2. We call the model with seasonality in transmissibility "Model 1". The model takes the form:

TABLE 3. Definition of the parameters in the modeling framework

Parameter	Meaning
Λ_d	Birth/recruitment rate of domestic birds
$\beta_{H_d}(t)$	Transmission rate of HPAI among domestic birds
$I_w(t)$	Number of infected wild birds
$f(I_w(t))$	Periodic source of infection from wild birds
μ_d	Natural death rate of domestic birds
ν_{H_d}	HPAI-induced mortality rate for domestic birds
$\delta(t)$	Decay rate of the virus
η	Shedding rate of the virus into the environment
Λ	Birth/recruitment rate of humans
β	Transmission coefficient of HPAI from birds to humans
μ	Natural death rate of humans
ν	Death rate of humans due to HPAI
ρ	Transmission rate of the free virus

$$M_1 \quad \begin{cases} \dfrac{dS_d}{dt} &= \Lambda_d - \beta_{H_d}(t) I_{H_d} S_d - \mu_d S_d, \\ \dfrac{dI_{H_d}}{dt} &= \beta_{H_d}(t) I_{H_d} S_d - (\mu_d + \nu_{H_d}) I_{H_d} \\ \dfrac{dS}{dt} &= \Lambda - \beta I_{H_d} S - \mu S \\ \dfrac{dI}{dt} &= \beta I_{H_d} S - (\mu + \nu) I \end{cases}$$

with positive initial conditions : $S_d(0), I_{H_d}(0), S(0), I(0) > 0$. Parameters of the model are described in Table 3.

The transmission rate $\beta_{H_d}(t)$ is assumed to be periodically forced. In particular, we take

$$\beta_{H_d}(t) = \kappa_1 \sin\left(\frac{2\pi}{365}(t + \omega_1)\right) + \kappa_2 \tag{3.1}$$

This form assumes 365-day periodicity and has amplitude κ_1, vertical shift κ_2, and phase shift ω_1 which are to be determined by fitting. This simple sinusoidal function is chosen for two reasons: (1) It has the advantage of simplicity and ease in computation; (2) In some cases this sinusoidal function may represent a linear transformation of a weather covariate [33]. We assume that $\kappa_1 \leq \kappa_2$ so that $\beta_{H_d}(t) \geq 0$ for all time.

3.2. **Seasonally introduced infections from wild birds.** The role of wild migratory birds in the global spread of H5N1 has been controversial and is still being investigated [44]. It appears that some wild migratory birds can be asymptomatic to HP H5N1 and

can carry the virus over long distances [35]. Outbreaks of HP H5N1 strains among wild birds are limited temporally and occur primarily during the winter and spring months. In Thailand, Keawcharoen *et al.* find that there is strong association between the outbreaks in wild birds and poultry. In particular, the authors find that the transmission efficiency of H5N1 among poultry flocks was 1.7 times higher in regions with infected wild birds in the given or the preceding month [20]. Prosser *et. al.* [35] also find connection between wild bird and poultry outbreaks but conclude that wild bird outbreaks follow poultry outbreaks. Both studies remark that whether the wild bird outbreak are a cause for the poultry outbreak or vice versa is difficult to ascertain.

We assume that seasonality in migratory patterns of wild birds could be another possible source for oscillations of H5N1 in poultry. Wild migratory birds move from their breeding grounds to their wintering grounds in the fall, potentially contacting local poultry during stopovers and at destination, and spreading the virus south along their migratory pathways [30]. We will capture a periodic introduction of HP H5N1 into poultry through one source term accounting for oscillatory wild bird→poultry transmission. We assume the incidence term of new infections coming from the wild birds to the poultry is given by $f(I_w(t))S_d$ where

$$f(I_w(t)) = \kappa_3 \sin\left(\frac{2\pi}{365}(t+\omega_2)\right) + \kappa_4.$$

The amplitude κ_3 and the vertical shift κ_4 satisfy the inequality $\kappa_3 \leq \kappa_4$ so that $f(I_w(t)) \geq 0$ for all time. This incidence term captures two possible scenarios of seasonality: (1) The number of infected wild birds is approximately constant but the contact rate $c(t)$ is oscillatory due to the migration patterns of the wild birds. In this case $f(I_w(t)) = c(t)I_w$; (2) The number of infected wild birds oscillates periodically $I_w(t)$ in general or from the perspective of poultry in wintering grounds. The seasonality in the number of infected birds can be a result of the seasonal breading patterns, as is in LPAI [4]. Seasonal breeding creates a new cohort of completely susceptible individuals, who then migrate possibly while infected to the wintering grounds where they contact the local poultry. Furthermore, we assume that the incidence of poultry is proportional to the product $f(I_w(t))S_d$. The function $f(I_w(t))$, as defined above, again has period of 365 days.

We call the model that incorporates seasonality introduced by wild bird migration "Model 2". Model 2 uses the same notation as Model 1 (see Table 3 and Table 2). Model 2 is given below.

$$M_2 \quad \begin{cases} \dfrac{dS_d}{dt} &= \Lambda_d - \beta_{H_d} I_{H_d} S_d - f(I_w(t))S_d - \mu_d S_d, \\ \dfrac{dI_{H_d}}{dt} &= \beta_{H_d} I_{H_d} S_d + f(I_w(t))S_d - (\mu_d + \nu_{H_d}) I_{H_d} \\ \dfrac{dS}{dt} &= \Lambda - \beta I_{H_d} S - \mu S \\ \dfrac{dI}{dt} &= \beta I_{H_d} S - (\mu + \nu) I \end{cases}$$

In Model 2 we assume that the transmission rate among poultry β_{H_d} is constant.

3.3. **Seasonality induced by environmental transmission of HP H5N1.** For low pathogenic avian influenza viruses and wild aquatic birds the role of the environmental transmission of the virus is well documented [39, 40, 45]. But LPAI viruses are transmitted through the fecal-oral route and shed primarily through the cloaca. HP H5N1 viruses, in contrast, are shed through the oropharynx and their main route of transmission is direct transmission. However, recently, studies indicate that the HP H5N1 viruses are becoming more stable in the environment. H5N1 viruses isolated from 2004 outbreaks in ducks survived at 37^oC for 6 days, compared with 2 days for viruses from the 1997 outbreak [50]. The increasing adaptation of the H5N1 virus to persistence in the environment suggests that this route of transmission of highly pathogenic viruses may be gaining importance [8, 49]. Indeed, a recent article focuses on the persistence of HP H5N1 on solid surfaces, chicken feces and soil depending on the ambient humidity and temperature [46]. Several studies investigate the persistence of the virus in different types of water and find that prolonged infectivity is possible [7, 28]. The dependence of the viral survival in the environment on temperature and humidity fluctuation may be introducing seasonality in H5N1 transmission among poultry. We model this type of seasonality through a periodic inactivation rate of the virus in the environment $\delta(t)$. To introduce the model, let $V(t)$ be the amount of virus in the environment measured in number of virions. We assume that the rate of transmissibility of the the virus is proportional to the free virus present in the environment and choose the force of infection as ρV. The model that involves seasonality in environmental transmission only is called Model 3. Model 3 is obtained from Model 1 by adding an equation modeling the dynamics of the virus in the environment and setting the transmission rate $\beta_{H_d}(t)$ to constant β_{H_d}. Birds shed virus into the environment at a rate η.

Model 3 is introduced below:

$$M_3 \quad \begin{cases} \dfrac{dS_d}{dt} &= \Lambda_d - \beta_{H_d} I_{H_d} S_d - \rho V S_d - \mu_d S_d, \\ \dfrac{dI_{H_d}}{dt} &= \beta_{H_d} I_{H_d} S_d + \rho V S_d - (\mu_d + \nu_{H_d}) I_{H_d} \\ \dfrac{dV}{dt} &= \eta I_{H_d} - \delta(t) V \\ \dfrac{dS}{dt} &= \Lambda - \beta I_{H_d} S - \mu S \\ \dfrac{dI}{dt} &= \beta I_{H_d} S - (\mu + \nu) I \end{cases}$$

We assume that the virus inactivation rate $\delta(t)$ is a sum of two components – one corresponding to solid environment, and another, corresponding to water. The two terms in $\delta(t)$ were used because of separate data for virus survival in soil and water and the relative contribution of each one is unknown.

$$\delta(t) = \alpha \left(\kappa_5 \sin\left(\frac{2\pi}{365}(t + \omega_3) \right) + \kappa_6 \right) + (1 - \alpha) \left(\kappa_7 \sin\left(\frac{2\pi}{365}(t + \omega_4) \right) + \kappa_8 \right)$$

where α is the fraction of solid environment. We identify the coefficients $\kappa_5, \ldots, \kappa_8$ in the next section.

Environmental transmission is well recognized route of transmission for LPAI viruses in wild birds. Mathematical models of environmental transmission, in addition to direct transmission, have shown significant impact of environmental transmission on the persistence of LPAI strains in wild birds [3, 4, 5, 37, 38]. The role of environmental pathways in the transmission of HPAI and its potential impact on the seasonality of H5N1 cases is partly what we address with this modeling framework.

4. Modeling framework and fixed parameter pre-estimation

To address what mechanism(s) may be responsible for the seasonality in the H5N1 cases in birds and humans and how we should model this seasonality, we consider a modeling framework that consists of a number of models, including Models 1,2 and 3 above. We then pre-estimate some of the parameters of the modeling framework and we fit each model in the framework to the cumulative number of human H5N1 cases.

4.1. **The modeling framework.**

We develop seven models that encompass different combinations of the drivers of seasonality introduced in Section 3. Model 1,2, and 3 are a part of that modeling framework. We also include models that incorporate pairs of drivers, all possible combinations, and a model that incorporates all three possible drivers of seasonality.

Model 1, 2, and 3 are as defined above. Model 4 (M_4) in that framework includes seasonality in the direct bird-to-bird transmission rate and seasonal introductions of H5N1 from wild birds, Model 5 (M_5) includes seasonal introductions of H5N1 from wild birds and seasonality from environmental transmission of H5N1, Model 6 (M_6) includes seasonality from bird-to-bird transmission of H5N1 and seasonality from environmental transmission, and finally Model 7 includes all three drivers. We call Model 7 (M_7) the *global model*. Transitions in the global model are illustrated in the flow-chart given in Figure 3.

The global model is given below:

$$M_7 \quad \begin{cases} \dfrac{dS_d}{dt} &= \Lambda_d - \beta_{H_d}(t) I_{H_d} S_d - f(I_w(t)) S_d - \rho V S_d - \mu_d S_d, \\ \dfrac{dI_{H_d}}{dt} &= \beta_{H_d}(t) I_{H_d} S_d + f(I_w(t)) S_d + \rho V S_d - (\mu_d + \nu_{H_d}) I_{H_d} \\ \dfrac{dV}{dt} &= \eta I_{H_d} - \delta(t) V \\ \dfrac{dS}{dt} &= \Lambda - \beta I_{H_d} S - \mu S \\ \dfrac{dI}{dt} &= \beta I_{H_d} S - (\mu + \nu) I \end{cases}$$

where the variables and the parameters are explained in Table 2 and Table 3.

Each of the models $M_1 - M_6$ is obtained from the global model by setting certain parameters equal to zero. In other words models $M_1 - M_6$ are nested in the global model. Table 4 gives a list of the models and how each model is obtained from the global model.

The total bird population size $N_d = S_d + I_{H_d}$ for the global model satisfies the differential equation

$$N_d'(t) = \Lambda_d - \mu_d N_d - \nu_{H_d} I_{H_d}.$$

FIGURE 3. Flow chart of the global model M_7

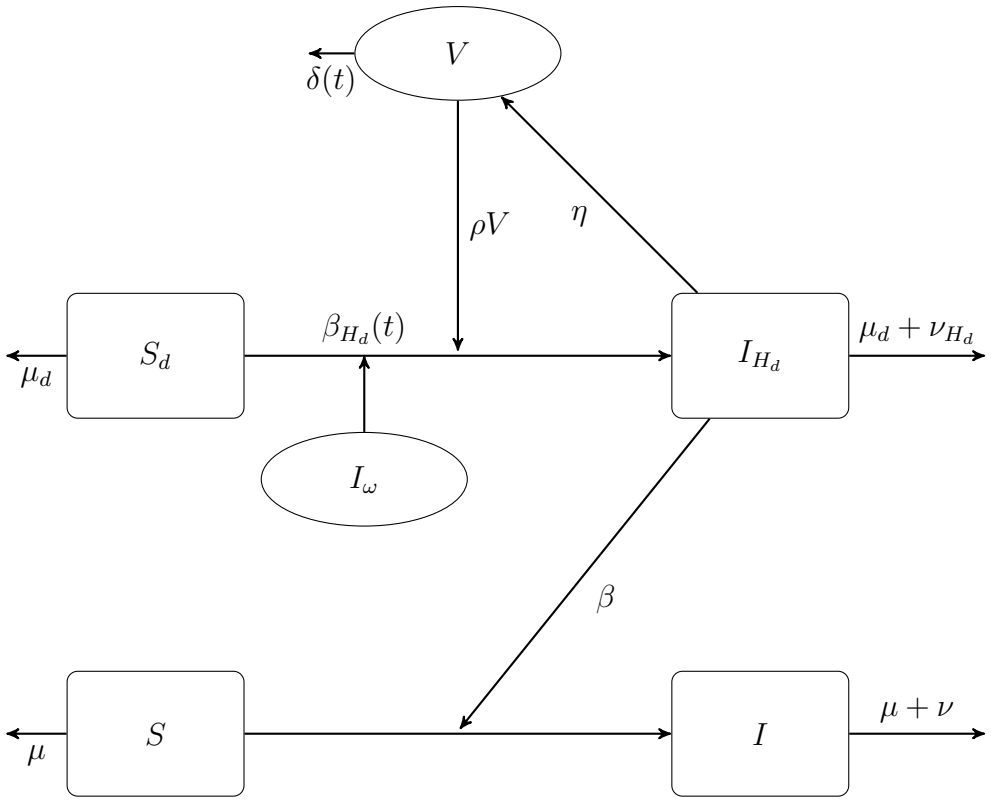

TABLE 4. Summary of the models in the modeling framework

Model	Drivers of seasonality	Reduction parameters
M_1	seasonal bird-to-bird transmissibility	$\eta = 0$, $\rho = 0$, $f(I_w) = 0$
M_2	seasonal introductions from wild birds	$\eta = 0$, $\rho = 0$,$\beta_{H_d}(t) = \beta_{H_d}$
M_3	seasonality from environmental transmission	$f(I_w) = 0$, $\beta_{H_d}(t) = \beta_{H_d}$
M_4	(1) seasonality in bird-to-bird transmission (2) seasonal introductions from wild birds	$\eta = 0$, $\rho = 0$
M_5	(2) seasonal introductions from wild birds (3) seasonality from environmental transmission	$\beta_{H_d}(t) = \beta_{H_d}$
M_6	(1) seasonality from bird-to-bird transmission (3) seasonality from environmental transmission	$f(I_w) = 0$
M_7	all three mechanisms	

This equation is not closed but it can be easily seen that the total bird population size satisfies the inequality

$$N_d'(t) \leq \Lambda_d - \mu_d N_d.$$

Hence, $\limsup_t N_d \leq \Lambda_d/\mu_d$. We will use this quantity as an approximation of the total bird population size in pre-estimating parameters. Similarly, the total human population size $N = S + I$ for the global model satisfies the differential equation

$$N'(t) = \Lambda - \mu N - \nu I.$$

This equation is also not closed but it can be easily seen that the total human population size satisfies the inequality

$$N'(t) \leq \Lambda - \mu N.$$

Hence, $\limsup_t N \leq \Lambda/\mu$. We will use this fraction as an approximation of the total human population size.

4.2. **Pre-estimating common parameters.** Even the simplest Model 1 has ten parameters and four initial conditions that may need fitting. Fitting that many parameters may make the problem sensitive to the initial conditions of the parameters and may result in rather large and unrealistic confidence intervals. To reduce the number of parameters fitted with each model, we pre-estimate some parameters.

4.2.1. *Pre-estimating demographic and infection-related parameters.* To estimate parameters, we need to set up units. We measure time t in days. Generally, we pre-estimate the demographic parameters for humans and poultry as well as the duration of infectious period, and we fit parameters related to the seasonal forcing and transmission rates. We first pre-estimate the parameters related to poultry. Commercial poultry is kept for about 2 years. Hence, $\mu_d = 1/(2 * 365)$ days^{-1}. The total world poultry population can be obtained from the Food and Agriculture Organization of the United Nations (FAO) [10]. FAO gives 20.4 billion poultry units in 2008 (1 poultry unit = 1 domestic bird, for example 1 chicken). We write the total poultry population size as $N_d = 2040$ counting this number in units of 10^7 individuals. Then $\Lambda_d \approx N_d \mu_d$. Hence, $\Lambda_d = 1020/365$ times 10^7 individuals per day. The duration of infectiousness in domestic birds is taken to be 10 days [18], that is $\nu_{H_d} = 0.1$ days^{-1}. We pre-estimate the human parameters in a similar way. Several sources give an average value of human lifespan. We take that to be 65 years [51], therefore $\mu = 1/(65 * 365)$ days^{-1}. World human population is approximately 6.5 billion. As before we consider $N \approx 65000$ in units of 10^5 people. That gives a value of $\Lambda = 1000/365$ births per day in units of 10^5 individuals. We assume that initially whole population is susceptible, thus $S(0) = 65000$, and set $I(0) = 0.00047$ in units of 10^5 people. Various sources [18, 48] give the mean duration of infection in humans of the bird-to-human avian influenza strain to be of 6-7 days. We take $\nu = 0.15$ days^{-1}.

4.2.2. *Pre-estimating parameters related to $\delta(t)$.* Viral clearance rate $\delta(t)$ is associated with 6 parameters. To reduce the number of parameters fitted, we pre-estimate $\kappa_5, \ldots, \kappa_8$. Parameters κ_5, κ_6 are associated with solid environment, and parameters κ_7, κ_8 are associated with water. Article [46] studied viral persistence on solid environment under different environmental conditions. Articles [7, 28] studied viral persistence in different types of water. We use the results of these articles to estimate high and low values of $\delta(t)$ which we denote by d, the decay rate of the virus. Then we estimate $\kappa_5, \ldots, \kappa_8$ by fitting a general sine function through the high and the low.

TABLE 5. High and low values of d for solid surfaces (chicken feces and soil) and water (pond water and seawater).

	Chicken feces	Soil	Pond water	Seawater
high	8.052 (low humidity)	5.42 (low humidity)	0.783 (20^oC)	1.223 (20^oC)
low	0.902 (high humidity)	0.55 (high humidity)	0.345 (10^oC)	0.466 (10^oC)

To find the high and the low of d for solid environment, which gives the interval in which δ ranges, we use Table 4 in [46]. We assume the virus decays at the exponential rate d so the amount of virus left in t days in

$$Q(t) = Q_0 e^{-dt}$$

where Q_0 is the inoculation size. From this formula we have that

$$d = \frac{1}{t} \ln \left(\frac{Q_0}{Q(t)} \right).$$

Article [46] uses inoculation size $2 * 10^6$ (see Table 1 in [46]). For solid surfaces we compute the high and low values of d for chicken feces and soil as these two substances are most often present on poultry farms. To compute the high value, we take experiment 1 with room temperature and low humidity for chicken feces (Table 4 in [46]) to be $Q(t) = 6.37 * 10^2$ for $t = 1$ day. From the formula above we have

$$d = \frac{1}{1} \ln \left(\frac{2 * 10^6}{6.37 * 10^2} \right) = 8.052$$

For the persistence of H5N1 in water we use the results in Table 2 in [7]. In Table 2 of [7], d is estimated from the regression coefficient of the linear regression model. We obtain the Table 5 for the low and high values of d. So the sinusoidal function for solid surfaces satisfies

$$0.55 \leq \kappa_5 \sin \left(\frac{2\pi}{365}(t + \omega_3) \right) + \kappa_6 \leq 8.052.$$

This gives $\kappa_5 = (8.052 - 0.55)/2 = 3.752$ and $\kappa_6 = (0.55 + 8.052)/2 = 4.301$. Similarly, for water environment, we have

$$0.345 \leq \kappa_7 \sin \left(\frac{2\pi}{365}(t + \omega_4) \right) + \kappa_8 \leq 1.223.$$

This gives $\kappa_7 = 0.439$ and $\kappa_8 = 0.784$.

This gives the following function $\delta(t)$:

(4.1)

$$\delta(t) = \alpha \left(3.752 \sin \left(\frac{2\pi}{365}(t + \omega_3) \right) + 4.301 \right) + (1-\alpha) \left(0.439 \sin \left(\frac{2\pi}{365}(t + \omega_4) \right) + 0.784 \right)$$

The parameters determined in this subsection are fixed and the same for all models and all simulations. Fixed parameters and their values are listed in Table 6.

TABLE 6. Fixed parameters in the models

Parameters	Fixed Value (Model 1- Model7)
Λ	1000/365
Λ_d	1020/365
μ	$1/(65*365)$
μ_d	$1/(2*365)$
ν	0.15
ν_{H_d}	0.1
$S(0)$	65000
$I(0)$	0.00047

5. Model fitting and results

To compare the models in the modeling framework, we fit each of the seven models to the data on human cases of H5N1. WHO gives data on the cumulative number of confirmed H5N1 human cases [52]. For the model selection, we use the data in the interval 01/01/05 through 12/31/09. WHO updates the number of cumulative number of H5N1 cases based on the countries reports; some months there are several reports and some months there are none. The first three data points in our data set read as

$$1 \quad 0.00047; \qquad 18 \quad 0.00050; \qquad 33 \quad 0.00055\,.$$

This means that prior to 01/01/05 the total number of H5N1 cases were 47 and on January 18^{th} the total number reached to 50 and on February 2^{nd} it was 55. There were several reports on January 2005, but we only used the report on January 18^{th}. We use approximately one data point per month from the available dataset. Because data is given as cumulative number of new cases, we fit the cumulative number of the human incidence $C(t)$ where

$$C(t) = \int_0^t \beta S(\tau) I_{H_d}(\tau) d\tau$$

to the given data. The cumulative data is smoother than the incidence data. The incidence is chaotic and fitting it with a deterministic model is challenging. On the other hand fitting cumulative data has its drawbacks. One of the main concerns is that the earlier infections have more weight than the incidences at later dates. But it is not clear how to weigh them.

5.1. **Fitting procedure.** We use MATLAB to fit the model. We use an optimization routine and perform least square fitting of $C(t)$ to the data. For each model we fit a different number of initial conditions and parameters which range between 6 and 15 (Table 8 gives the parameters to be fitted in each model). The optimization procedure minimizes the least square distance

$$SSR = \sum_{i=0}^{n} |C(t_i) - y_i|^2 \tag{5.1}$$

where y_i is the cumulative number for the given time t_i, provided by WHO. The differences $C(t_i) - y_i$ are called *residuals*, and the *sum of squares of the residuals* is denoted by SSR. For each given set of values of the fitted parameters, we use an ODE solver to solve the differential equation system. We found out that stiff solvers in MATLAB

perform better with the optimization routines, so we used MATLAB routines ode15s and ode23s.

We fitted the data to the models using least square fit routine (*lsqcurvefit*) in MATLAB R2010b. This nonlinear curve fitting routine (*lsqcurvefit*) has two algorithms as options: " trust-region-reflective" and "levenberg-marquardt". Both of these numerical methods are iterative procedure, thus it is crucial to define initial values for each parameters. Since, *lsqcurvefit* finds local minima, if the initial values of the parameters are not close to the global minimum, the routine can not find the minimum (may find a bad local minimum). We find manual fitting helpful in defining the initial values. We performed the manual fitting in the following way, we first solve (numerically) the ODE model with given initial parameters, if the solution fits visually well the data, then we used these values as initial values in the nonlinear least square routine. We also used MultiStart which is a function in the new Global Optimization Toolbox (first launched in Matlab 2010 b) to vary the initial values of the parameters to wide range to ensure that we obtain the global minimum. However, this has not led to any better solutions. In our experience we find the manual fitting more helpful in determining the initial values. Table 7 lists the initial parameter values used in our fitting. We repeated the fitting procedure as many times as needed till the fitted parameters has not changed. That is, till the difference between the two consecutive parameter is less than the tolerance value of 10^{-15}. Matlab's default value is 10^{-6}, and we adjusted it to a value close to machine epsilon since our parameter values are very small to begin with.

We require the fitted parameters to be positive. We also require that

$$\beta_{H_d}(t) \geq 0 \quad \text{and} \quad f(I_w(t)) \geq 0.$$

The *lsqcurvefit* routine only allows bound constraints and does not allow any nonlinear constraints such as above. We implement the positivity of $\beta_{H_d}(t)$ and $f(I_w(t))$ by setting

$$\kappa_1 \leq \kappa_2 \quad \text{and} \quad \kappa_3 \leq \kappa_4 \,.$$

We notice that we can improve the sum of square residuals (SSR) by using the best fit parameters as initial values in the next step. We repeat this process until there are no further improvements in the SSR.

5.2. **Results of the fitting.** The first result from fitting each model was that the fitting produced parameter set for which each model best fits the data. Table 8 gives the values of the best fitted parameters. We note that most parameters vary little from model to model.

The main objective of this research is to find what type of mechanism(s) generates the oscillations of the number of human and bird cases of H5N1 as well as to find a model that models well these cases. To achieve this goal, we compare the models based on how well each model fits the data. If we were fitting the same number of parameters for each model, we can do the comparison based on the SSR error – the model with the smallest SSR would be the best model. However, we fit a different number of parameters for each model. In this case the comparison of the models, also referred to as model selection, is performed based on the Akaike Information Criterion (AIC). Akaike developed a method for comparing models based on their Kullback-Leibler distance (information) between the fitted model and the true unknown model that actually generated the data.

TABLE 7. Initial parameter values used in fitting

Parameters	Model 1	Model 2	Model 3	Model 4	Model 5	Model 6	Model 7
κ_1	$5.5 * 10^{-6}$	-	-	$4.9 * 10^{-6}$	-	$5. * 10^{-6}$	$4.92 * 10^{-6}$
κ_2	$5.35 * 10^{-5}$	-	-	$5.1 * 10^{-5}$	-	$5 * 10^{-5}$	$5.14 * 10^{-5}$
κ_3	-	$5 * 10^{-6}$	-	$4 * 10^{-7}$	$5 * 10^{-6}$	-	$5.9 * 10^{-7}$
κ_4	-	$8 * 10^{-6}$	-	$4.10 * 10^{-7}$	$8 * 10^{-6}$	-	$5.9 * 10^{-7}$
ω_1	127	-	-	127	-	127	127
ω_2	-	80	-	80	80	-	80
ω_3	-	-	80	-	80	0.97	7.26
ω_4	-	-	130	-	146	147	146
β	$2.3 * 10^{-11}$	$5 * 10^{-8}/365$	$1.9 * 10^{-11}$	$2.2 * 10^{-11}$	$2.2 * 10^{-11}$	$2.0 * 10^{-11}$	$2.3 * 10^{-11}$
β_{H_d}	-	0.03/365	$5.2 * 10^{-5}$	-	$2.2 * 10^{-5}$	-	-
α	-	-	10^{-4}	-	10^{-4}	0.6	0.61
ρ	-	-	10^{-6}	-	10^{-6}	$6.0 * 10^{-12}$	$1.7 * 10^{-11}$
η	-	-	10^{-5}	-	10^{-5}	$6.39 * 10^{-4}$	$4.65 * 10^{-3}$
$S_d(0)$	1940.6	3750	1978.55	2004	3750	1981.19	2015.17
$I_{H_d}(0)$	2.0698	0.2	2.06	1.8	0.2	2.02	1.70
$V(0)$	-	-	10^{-5}	-	10^{-3}	0.26	0.23

TABLE 8. Fitted parameters in the models

Parameters	Model 1	Model 2	Model 3	Model 4	Model 5	Model 6	Model 7
κ_1	$5.35 * 10^{-6}$	-	-	$5.42 * 10^{-6}$	-	$5.01 * 10^{-6}$	$4.92 * 10^{-6}$
κ_2	$5.27 * 10^{-5}$	-	-	$5.19 * 10^{-5}$	-	$5.25 * 10^{-5}$	$5.14 * 10^{-5}$
κ_3	-	$1.46 * 10^{-5}$	-	$2.5 * 10^{-11}$	$3.27 * 10^{-6}$	-	$5.88 * 10^{-7}$
κ_4	-	$2.85 * 10^{-5}$	-	$3.57 * 10^{-7}$	$6.93 * 10^{-6}$	-	$5.88 * 10^{-7}$
ω_1	107.75	-	-	106.34	-	125.81	126.71
ω_2	-	79.99	-	72.70	79.99	-	80.11
ω_3	-	-	89.95	-	$1.19 * 10^{-3}$	0.97	7.28
ω_4	-	-	115.39	-	145.99	149.80	145.77
β	$1.9 * 10^{-11}$	$2.5 * 10^{-11}$	$1.4 * 10^{-12}$	$2.1 * 10^{-11}$	$1.28 * 10^{-10}$	$2.0 * 10^{-11}$	$2.3 * 10^{-11}$
β_{H_d}	-	$2.37 * 10^{-5}$	0.56	-	$1.27 * 10^{-5}$	-	-
α	-	-	0.09	-	0.17	0.59	0.61
ρ	-	-	$6.72 * 10^{-3}$	-	$2.37 * 10^{-6}$	$1.0 * 10^{-12}$	$1.7 * 10^{-11}$
η	-	-	0.04	-	$2.83 * 10^{-6}$	$6.36 * 10^{-4}$	$6.76 * 10^{-3}$
$S_d(0)$	1975.27	2928.49	$9 * 10^{-4}$	2001.53	3781.88	1979.78	2015.17
$I_{H_d}(0)$	1.77	0.5275	99.81	1.55	$8.49 * 10^{-3}$	2.0	1.70
$V(0)$	-	-	20.58	-	0.08	0.26	0.22

TABLE 9. Model selection parameters: SSR, AICc, Δ_i.

Model	Parameters	SSR	AIC	AIC_c	w_i	$\Delta AICc$
M_1	$\kappa_1, \kappa_2, \omega_1, \beta$ $S_d(0), I_{H_d}(0)$	$2.2530 * 10^{-7}$	$-1.8935 * 10^3$	$-1.8923 * 10^3$	0.9707	0.0
M_2	$\kappa_3, \kappa_4, \omega_2, \beta_{H_d}$ $\beta, S_d(0), I_{H_d}(0)$	$1.4864 * 10^{-6}$	$-1.7104 * 10^3$	$-1.7088 * 10^3$	$1.3822 * 10^{-40}$	183.5
M_3	$\beta, \beta_{H_d}, \alpha, \omega_3, \omega_4$ $\rho, \eta, S_d(0)$ $I_{H_d}(0), V(0)$	$6.1751 * 10^{-6}$	$-1.5677 * 10^3$	$-1.5646 * 10^3$	$1.1662 * 10^{-71}$	327.7
M_4	$\kappa_1, \kappa_2, \kappa_3, \kappa_4,$ $\beta, S_d(0), I_{H_d}(0)$ ω_1, ω_2	$2.245 * 10^{-7}$	$-1.8879 * 10^3$	$-1.8853 * 10^3$	0.0293	7.0
M_5	$\kappa_3, \kappa_4, \alpha, \omega_2, \omega_3$ $\omega_4, \rho, \eta, \beta, \beta_{H_d}$ $S_d(0), I_{H_d}(0)$ $V(0)$	$1.4035 * 10^{-6}$	$-1.7039 * 10^3$	$-1.6987 * 10^3$	$8.8588 * 10^{-43}$	193.6
M_6	$\kappa_1, \kappa_2, \beta, \alpha, \omega_1$ $\omega_3, \omega_4, \rho, \eta, S_d(0)$ $I_{H_d}(0), V(0)$	$2.6693 * 10^{-7}$	$-1.8653 * 10^3$	$-1.8608 * 10^3$	$1.4026 * 10^{-7}$	31.5
M_7	$\kappa_1, \kappa_2, \kappa_3, \kappa_4, \beta$ $\alpha, \omega_3, \rho, \eta, S_d(0)$ $I_{H_d}(0), V(0)$ $\omega_1, \omega_2, \omega_4$	$2.6751 * 10^{-7}$	$-1.8591 * 10^3$	$-1.8522 * 10^3$	$1.9032 * 10^{-9}$	40.1

AIC, in fact, applies when the ratio of the number of data points to the number of parameters fitted is large enough. If this ratio is not large, then a corrected version of AIC is used, denoted by AICc. To compare the models, we compute AICc for each model, based on the formula [6]:

$$AIC_c = n \ln\left(\frac{SSR}{n}\right) + 2K + \frac{2K(K+1)}{n-K-1} \tag{5.2}$$

where SSR is the sum of squares of the residuals for the fitting of the given model, n is the number of data points, and K is the number of parameters fitted plus one.

The smaller the AICc for a model, the better that model describes the data. In order to chose the "best" model, we first calculate the AICc values for each of the seven models, then choose the model with the smallest AICc value. Then we say that this model with the least AICc value is the "best" model in the sense that it is the closest to the true unknown model. AICc estimates relative support that the data gives for a model. To estimate that support and to compare the models, we calculate the differences between the AICc value of a given model to the AICc value of the "best" model. For instance, if $AICc_{\min}$ is the AICc of the the best fitted model, to compare model i to the best fitted model we compute:

$$\Delta_i AICc = AICc_i - AICc_{\min} = \Delta_i$$

The main parameters needed for model comparison and selection are listed in Table 9. Looking at that table, we see that AIC and AICc are approximately the same which means that we are using large enough set of data for the number of parameters being estimated. We also note that the values of the AIC and AICc are negative but this stems from the small SSR error.

If all models are nested, that is, model M_i can be obtained from model M_{i+1} by setting the value of certain parameter(s) (usually to zero). As a rough rule of thumb for nested models some models, depending on their AICc difference from the "best" model, might still have support in the data, while other can be completely ruled out. The rough principles that apply in that selection are as follows [6]: Models for which $0 \leq \Delta_i \leq 2$ have substantial support in the data and should receive consideration in making inferences. Models for which $4 \leq \Delta_i \leq 7$ have considerably less support but cannot be ruled out. Models for which $\Delta_i > 10$ have either essentially no support and might be omitted from further consideration or at least fail to explain some substantial structural variation in the data. If the models being compared are not nested, then these boundaries might be somewhat larger.

Our modeling framework does not consist only of nested models but there are subsequences of models that are nested. The sequences of nested models that are of interest are

$$M_1 \hookrightarrow M_6 \hookrightarrow M_7$$

and

$$M_1 \hookrightarrow M_4 \hookrightarrow M_7$$

Table 9 shows that the model with the lowest AICc is Model 1. Models 1, Model 6, Model 7 form a sequence of nested models. Thus Table 9 and the above rule imply that Model 6 and Model 7 can be disregarded as they do not explain the data as well as Model 1. Furthermore, Model 1 is nested in Model 4 which is the second best. The $\Delta_4 = 7$, we can not disregard Model 4. It has some support from the data.

Another approach to gauge the relative support the data give to the various models in the modeling framework, particularly when the models are not all nested, is the Akaike weights. The Akaike weight for Model i is defined as

$$w_i = \frac{e^{-\Delta_i/2}}{\sum_{j=1}^{8} e^{-\Delta_j/2}}.$$

Models whose Akaike weights sum to $\sum w_i \geq 0.95$ give the confidence set of models that explain the given data [6]. In our case $w_1 > 0.97$ (see Table 9), so Model 1 explains the data well enough that no other models are needed in the confidence set.

The fit the best model gives to the data is given in Figure 4. To compare the best fitted model, we changed the Model 1 by taking $\beta_{H_d}(t) = \beta_{H_d}$ to be constant so that the new version has no seasonality. We fitted the new version of Model 1 with no seasonality and the fitting resulted with higher residual norm (results are not shown). We plot the fit in Figure 5for comparison.

6. Mathematical properties of the best fitted model

The best fitted model is a very simple SI epidemic model with periodic transmission rate and disease induced mortality. Despite its simplicity, the best fitted model - Model 1, given by equation (3.1), has the property of exhibiting complex behavior. Seasonally

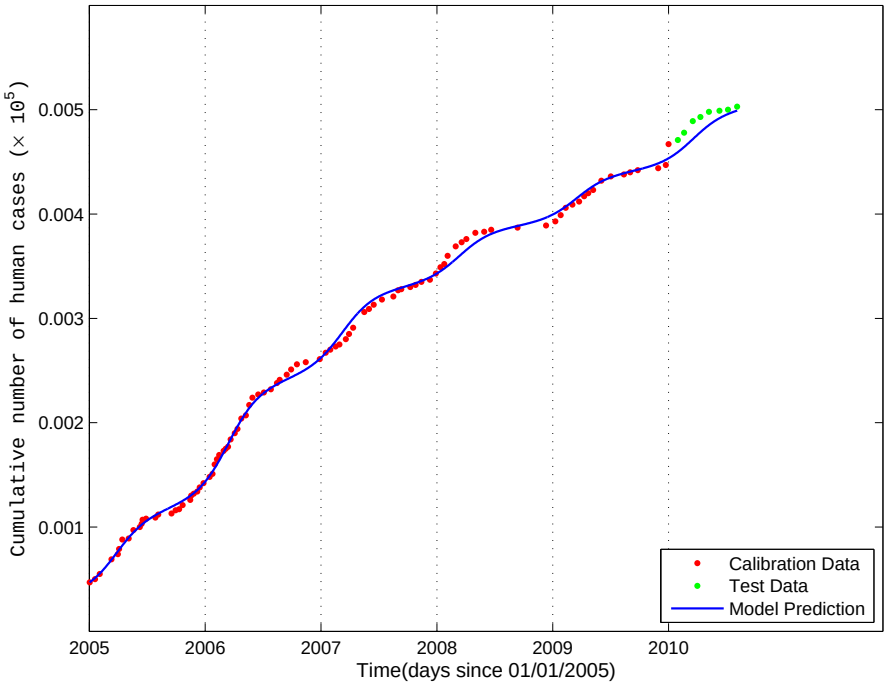

FIGURE 4. Predictions of Model 1 and their fit to data.

forced SIR and SEIR models with periodicity in the transmission rate have a long history of being studied as models of recurrent epidemics with childhood diseases playing a major role in that set. Aaron and Schwartz [1] find period doubling bifurcations in the SEIR model. More recently, the presence of chaos has also been established in SIR and SEIR models [26, 36, 29]. Seasonally forced SI models, however, have received little attention. We consider the best fitted model (3.1) and we address the question: In the simplest epidemic models with seasonal forcing in the transmission rate, when does the complexity arise?

6.1. **The reproduction number.** Computing the reproduction number explicitly is not possible for most of the more complex epidemic models [24, 42]. The reproduction number for Model 1 (3.1), however, can be explicitly computed and is given by

$$\mathcal{R}_0 = \frac{\Lambda_d \int_0^{365} \left[\kappa_1 \sin\left(\frac{2\pi}{365}(t+\omega_1)\right) + \kappa_2\right] dt}{365\mu_d(\mu_d + \nu_{H_d})} \tag{6.1}$$

The integral in (6.1) can be simplified to $365\kappa_2$, giving the simpler form for $\mathcal{R}_0$.

$$\mathcal{R}_0 = \Lambda_d \kappa_2 / \mu_d(\mu_d + \nu_{H_d})$$

To see the expression (6.1), notice that Model 1 (3.1) has a time-independent disease-free equilibrium $\mathcal{E}_0 = \left(\frac{\Lambda_d}{\mu_d}, 0\right)$. The equation for I_{H_d} linearized around the disease-free

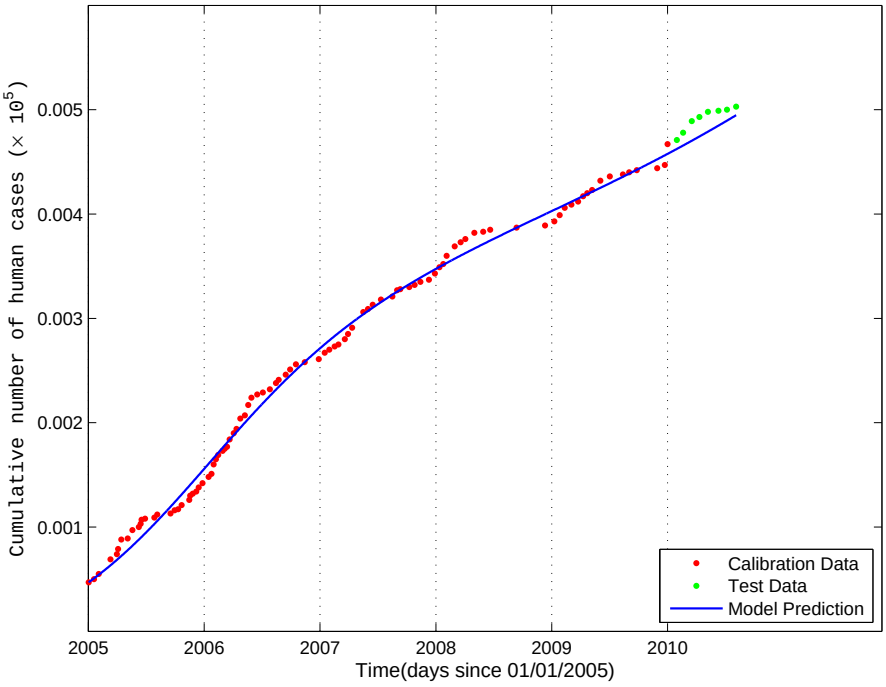

FIGURE 5. Predictions of a version of Model 1 with no seasonality and their fit to data.

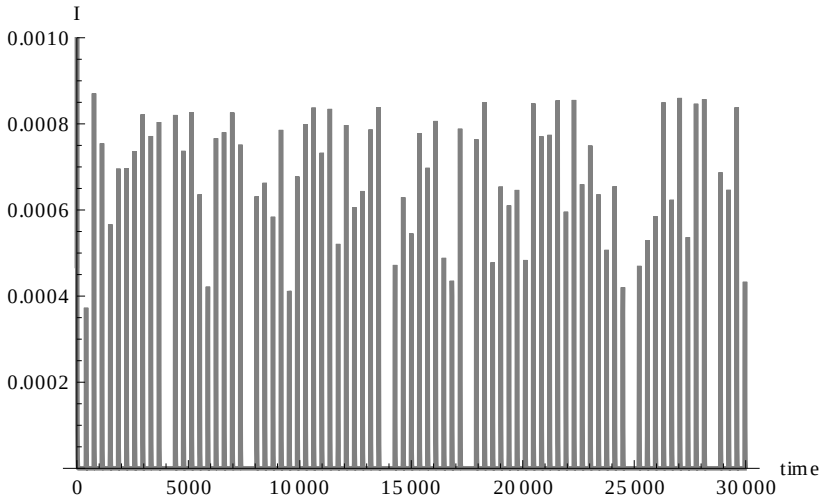

FIGURE 6. Plot of I with respect to time. I clearly persists and is not going to zero if $\beta_{H_d}(t)$ is not necessarily positive. The transmission rate $\beta_{H_d}(t)$ is given by formula (3.1) with $\kappa_1 = 0.005111486$ and $\kappa_2 = 0.00032621758$, $\nu_{H_d} = 0.7$, $\omega_1 = 127$, $\beta = 2.1 * 10^{-11}$. Other parameters are as obtained for the best fitted Model 1. The reproduction number is $\mathcal{R}_0 = 0.95$.

equilibrium $I_{H_d}(t) = 0 + i(t)$ splits from the linearized equation for S and it is given by

$$i'(t) = \beta_{H_d}(t)\frac{\Lambda_d}{\mu_d}i(t) - (\mu_d + \nu_{H_d})i(t). \tag{6.2}$$

If $\mathcal{R}_0 < 1$ then $\lim_{t\to\infty} i(t) = 0$. If, however, $\mathcal{R}_0 > 1$, then $i(t) \to \infty$. We have established the following result:

Proposition 6.1. *Assume $\beta(t) \geq 0$. The disease-free equilibrium $\mathcal{E}_0$ of the system (3.1) is locally asymptotically stable if $\mathcal{R}_0 < 1$. If $\mathcal{R}_0 > 1$, then the disease-free equilibrium $\mathcal{E}_0$ is unstable.*

In fact a stronger result is possible. If $\beta(t) \geq 0$ then the disease-free equilibrium is globally asymptotically stable.

Proposition 6.2. *Assume $\beta(t) \geq 0$. The disease-free equilibrium $\mathcal{E}_0$ of the system (3.1) is globally asymptotically stable if $\mathcal{R}_0 < 1$.*

Proof. Let $\epsilon > 0$ be small enough. We notice that $N_d(t) \leq \hat{N}_d(t)$ where $\hat{N}_d$ is the solution of the following equation:

$$\hat{N}_d' = \Lambda_d - \mu_d \hat{N}_d.$$

We consider the more difficult case when $\hat{N}_d(0) > \frac{\Lambda_d}{\mu_d}$. Then, we can find $t_0 > 0$ such that $\hat{N}_d(t) < \frac{\Lambda_d}{\mu_d} + \epsilon$ for all $t > t_0$. From $S_d(t) \leq N_d(t) \leq \hat{N}_d(t)$ we have that for every $t > t_0$

$$I_{H_d}' \leq \left(\beta_{H_d}(t)\left(\frac{\Lambda_d}{\mu_d} + \epsilon\right) - (\mu_d + \nu_{H_d})\right) I_{H_d} \tag{6.3}$$

In the above inequality we have taken into account that $\beta(t) \geq 0$. Since $\mathcal{R}_0 < 1$ we can choose $\epsilon > 0$ is small enough, so that

$$\int_0^{365} \left(\beta_{H_d}(t)\left(\frac{\Lambda_d}{\mu_d} + \epsilon\right) - (\mu_d + \nu_{H_d})\right) dt < 0.$$

Integrating (6.3) from t_0 to t we have

$$I_{H_d}(t) \leq I_{H_d}(t_0) e^{\int_0^{t_0}\left(\beta_{H_d}(t)\left(\frac{\Lambda_d}{\mu_d}+\epsilon\right)-(\mu_d+\nu_{H_d})\right)dt} e^{-\int_0^t\left(\beta_{H_d}(s)\left(\frac{\Lambda_d}{\mu_d}+\epsilon\right)-(\mu_d+\nu_{H_d})\right)ds}.$$

It is easy to see that $I_{H_d} \to 0$ as $t \to \infty$. □

If time-dependent transmission rate is not positive, there are subthreshold non-zero solutions (see Figure 6).

6.2. **Emergence of complex dynamics.** Despite its simplicity, model (3.1) is capable of producing very complex dynamical behavior. With the best fitted parameters, the reproduction number is $\mathcal{R}_0 = 1.06$ and the solutions of the system converge to a periodic solution. We increase κ_1 and κ_2 so that the reproduction number is larger but still within realistic biological boundaries, so when we increase ν_{H_d} for period doubling, the reproduction number does not drop below one. Then, we can observe period doubling, that is a period four solution emerging from a period two solution, a period eight solution emerging from a period four solution and etc. Eventually, the solutions of Model 1 exhibit chaotic behavior (see Figure 7).

What drives this complex dynamical behavior in a model as simple as Model 1? From one side this is the time-periodic transmission rate $\beta_{H_d}(t)$. If the transmission rate is

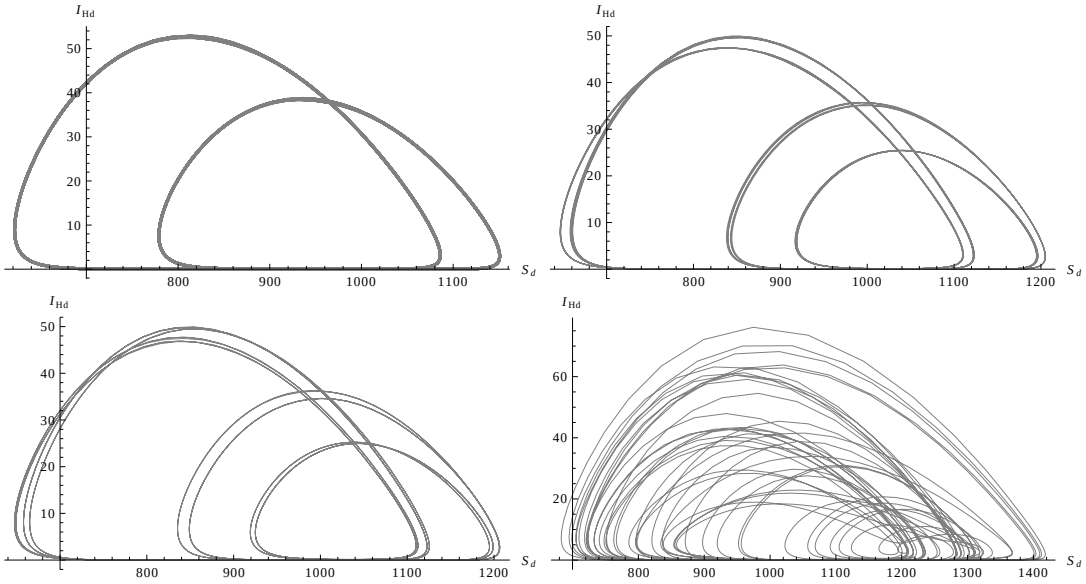

FIGURE 7. Series of figures showing a period two solution, period four solution, period eight solution, and chaos in Model 1. All parameters are as the best fitted parameters for Model 1, except $\kappa_1 = 0.00005111486$ and $\kappa_2 = 0.00032621758$. The values of ν_{Hd} are $\nu_{Hd} = 0.3, 0.315, 0.3155, 0.35$.

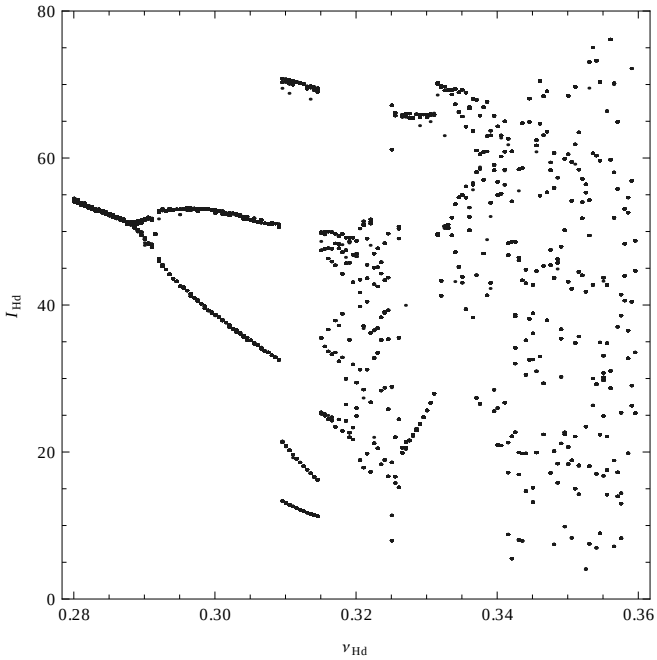

FIGURE 8. Chaos bifurcation diagram for Model 1. As ν_{H_d} increases the system undergoes period doubling and transition to chaos. Parameters set as the best fitted parameters except κ_1 and κ_2. $\kappa_1 = 0.00005111486$ and $\kappa_2 = 0.00032621758$.

constant, that is if $\kappa_1 = 0$, then the autonomous version of Model 1 has a unique endemic equilibrium which is globally stable. If, however, the model is non-autonomous, then the parameter that drives the complex chaotic behavior is the disease-induced mortality ν_{H_d}. Indeed, if $\nu_{H_d} = 0$, then the resulting system (3.1) reduces to a single equation of Bernoulli type:

$$I'_{H_d} = \beta_{H_d}(t)(N_d(t) - I_{H_d})I_{H_d} - \mu_d I_{H_d} \tag{6.4}$$

where N_d is the solution of the equation $N'_d = \Lambda_d - \mu_d N_d$. The Bernoulli equation can be solved via the substitution $y = 1/I_{H_d}$. The solution is given by

$$I_{H_d} = \frac{I_{H_d}(0)}{e^{-\int_0^t r(s)ds} + I_{H_d}(0)\int_0^t e^{-\int_s^t r(\tau)d\tau}\beta_{H_d}(s)ds}$$

where $r(t) = \beta_{H_d}(t)N_d(t) - \mu_d$. Equation (6.4) has a unique periodic solution that attracts all other solutions. That result follows from Theorem 3.1 in [25] in the case when $N_d(0) = \Lambda_d/\mu_d$. If $N_d(0) \neq \Lambda_d/\mu_d$, the result can be extended using the fact that $N_d(t) \to \Lambda_d/\mu_d$ as $t \to \infty$ and a comparison principle (see also [41]). Therefore, for $\nu_{H_d} = 0$ model (3.1) does not exhibit chaotic behavior. As ν_{H_d} increases the system undergoes period doubling and transition to chaos. This behavior is illustrated in the chaos bifurcation diagram of Model 1 (3.1) (see Figure 8). We conclude that given periodic contact rate or susceptibility, increasing the disease-induced virulence, in other words decreasing the infectious period, may destabilize the system. Control measures applied to poultry, such as culling and vaccination, often work to decrease the infectious period. Although, for the best fitted parameters decreasing the infectious period will only lead to the elimination of the disease, for higher reproduction number destabilization of the system and chaos may occur before elimination.

7. Discussion

The question "What drives the seasonality in influenza A?" is a complex question that should be addressed through integrative tools. Even for human influenza A, with human influenza being extensively studied, this question has not received a definite answer. It is possible that symbiosis among multiple mechanisms brings this coherent dynamic behavior. As science has not identified the mechanisms that produce influenza A's seasonality, modeling the seasonality is so much more challenging.

Avian influenza H5N1 has been infecting humans regularly since 2003. The number of cases in humans and the poultry outbreaks have been exhibiting seasonality, very much like the one human influenza exhibits in temperate climates in the Northern hemisphere, that is, the number of human cases and poultry outbreaks display a surge in the winter months, December-April, and are relatively minimal during the summer months. Because avian influenza involves multiple species, tracing the roots of this seasonality is much more difficult. On the other hand, we need avian influenza models that faithfully reflect that seasonality, something that the early models on avian influenza completely neglected.

In this paper we address the question "How do we model the seasonality of H5N1 influenza?". We first examined the likelihood that some climatic factor, such as temperature or rainfall, may be associated with seasonality. However, data suggests that the association may be possible for specific regions or countries but no such association

exists across all affected countries. One potential exception is the number hours of sunlight per day which across all countries tends to peak in the summer and be low during the winter months. We assume that the number of hours of sunlight may be responsible for fluctuations in host susceptibility but further research may be necessary to elucidate the role of sunlight in the H5N1 seasonality.

We model climatic influence, if one exist, indirectly through periodicity in the coefficients. We hypothesize three potential drivers of seasonality in H5N1: (1) seasonality in the domestic bird-to-bird transmission; (2) seasonality in the transmission from wild birds to domestic birds; (3) seasonality stemming from environmental transmission. We consider seven models involving these three potential mechanisms and their combinations. We fit the seven models to the cumulative number of human H5N1 cases and compare their fit using the corrected Akaike Information Criterion (AICc). We find that the model that involves seasonality in the domestic bird-to-bird transmission (Model 1) fits the data best – significantly better than all other models. More precisely, our best fitted model suggest that the seasonality occurs in the one of the processes building the transmission rate: host susceptibility, host infectivity, or the contact rate. Hence, our best fitted model suggests, in agreement with climatic data, that seasonality in bird susceptibility may be an explanation for the observed periodicity in H5N1 cases. Model 4 which combines seasonality from bird-to-bird transmission and seasonal introductions from wild birds also received considerable support from the data and cannot be neglected as a potential modeling tool.

We compute a reproduction number for the best fitted model. The value of the reproduction number with the best fitted parameters of Model 1 is $\mathcal{R}_0 \approx 1.06$. This value of the reproduction number is significantly smaller than other estimates of the reproduction number of H5N1. For instance, Lucchetti *et al* [23] uses fitting to the cumulative number of human data and estimates a reproduction number for high pathogenic influenza $\mathcal{R}_0 = 2.72$. Applying various methods to a number of poultry outbreaks, Ward *et al.* [43] obtains reproduction numbers in the range 1.95-2.68. Bouma *et al.* estimates the reproduction number of H5N1 in experimental studies with mean $\mathcal{R}_0 = 1.6$ [2]. Compared to most existing estimates the estimate we obtain here is on the low side. However, it should be noted that a significant portion of the data that we use to obtain this value of the reproduction number is after 2006 when vaccination in poultry was introduced. Hence, the reproduction number we compute here, in effect is the controlled reproduction number, which can be expected to be much smaller.

Mathematically, our best fitted model is a very simple SI epidemic model with disease-induced mortality and a periodic transmission rate. For the best fitted parameters the model converges to a periodic solution. Yet, this simple model allows for realistic values of the parameters very complex dynamics. We find period doubling and transition to chaotic behavior. The parameter that drives this behavior is the virulence. If the disease-induced mortality (virulence) is zero, the resulting simpler model converges to a periodic solution, independently of the remaining parameters. The increase of the virulence destabilizes the system and drives chaotic behavior in that simple epidemic model with periodic transmission rate.

Acknowledgments

Authors acknowledge the support from NSF grant DMS-1220342.

References

[1] J.L. Aaron, I.B. Schwartz, Seasonality and period-doubling bifurcations in an epidemic model, *JTB* **110** (1984), p. 665-679.

[2] A. Bouma, I. Claassen, K. Natih, D. Klinkenberg, C. A. Donnelly, G. Koch, M. van Boven, Estimation of transmission parameters of H5N1 avian influenza virus in chickens, *PLoS Pathogens* **5(1)** (2009), e1000281.

[3] R. Breban, J.M. Drake, P. Rohani, A general multi-strain model with environmental transmission: Invasion conditions for disease-free and endemic states, *JTB* **264** (2010), p. 729-736.

[4] R. Breban, J.M. Drake, D.E. Stallknecht, P. Rohani, The role of environmental transmission in recurrent avian influenza epidemics, *PLoS Comp. Biol.* **5(4)** (2009), e1000346.

[5] R. Breban, J.M. Drake, D.E. Stallknecht, P. Rohani, Environmental transmission of low pathogenicity avian influenza viruses and its implications for pathogen invasion, *PNAS* **106** (2009), p. 10365-10369.

[6] K.P. Burnham, D.R. Anderson, Model selection and multimodel inference: A practical information-theoretic approach, 2^{nd} edition, Springer, 2002.

[7] K. Domanska-Blicharz, Z. Minta, K. Smietanka, S. Marche, T. van den Berg, H5N1 high pathogenicity avian influenza virus survival in different type of water, *Avian Dis.* **54** (2010), p. 734-737.

[8] L.Q. Fang, S.J. de Vlas, S. Liang, C.W.N. Looman, P. Gong, B. Xu *et al.*, Environmental factors contributing to the spread of H5N1 avian influenza in mainland China, *PLoS One* **3(5)** (2008), e2268.

[9] S.R. Fereidouni, E. Starick, M. Beer, D. Kalthoff *et al.*, Highly pathogenic avian influenza virus infection of mallards with homo- and heterosubtypic immunity induced by LPAI viruses, *PLoS One* **4 (8)**, (2009),e6705.

[10] Food and Agriculture Organization, FAO Statistics, CountrySTAT, http://www.fao.org/.

[11] Food and Agriculture Organization of the United Nations, Animal Production and Health Division
http://www.fao.org/avianflu/en/overview.htm

[12] A. Petrini, OIE, A Global situation: HPAI outbreaks in poultry- a synthesis of country reports to the OIE, Technical Meeting on HPAI and Human Infection, June 2007.

[13] C. Fuhrmann, The effects of weather and climate on the seasonality of influenza: what we know and what we need to know, *Geography Compass* **4/7** (2010), p. 718-730.

[14] S. Herfst et al., Airborne transmission of Influenza A/H5N1 virus between ferrets, *Science*, 336:1534-41, (2012).

[15] A.W. Hampson, Epidemiological data on influenza in Asian countries, *Vaccine* **17** (1999), p. S19 -S23.

[16] S. Iwami, Y. Takeuchi, X. Liu Avian-human influenza epidemic model, *Math. Biosci.* **207** (2007), p. 1-25.

[17] S. Iwami, Y. Takeuchi, A. Korobeiniov, X. Liu, Prevention of avian influenza epidemic: What policy should we choose?, *JTB* **252**, (2008), p. 732-741.

[18] S. Iwami, Y. Takeuchi, X. Liu, Avian flu pandemic: Can we prevent it?, *JTB* **257**, (2009), p. 181-190.

[19] S. Iwami, T. Suzuki, Y. Takeuchi, Paradox of vaccination: Is vaccination really effective against avian flu epidemics? *PLoS One* **4 (3)** (2009), e4915.

[20] J. Keawcharoen, J. van den Broek, A. Bouma, T. Tiensin, A. D.M.E Osterhaus, H. Heesterbeek, Wild birds and increased transmission of highly pathogenic avian influenza (H5N1) among poultry, Thailand, *EID* **17 (6)** (2011), p. 1016-1022.

[21] K.S. Li, Y. Guan, J. Wang, G.J.D. Smith, K.M. Xu, L. Duan, *et al.*, Genesis of a highly pathogenic and potentially pandemic H5N1 influenza virus in eastern Asia, *Nature* **430** (2004), p. 209213.

[22] E. Lofgren, N. H. Fefferman, Y. N. Naumov, J. Gorski, E. N. Naumova, Influenza seasonality: underlying causes and modeling theories, *J. Virology*, **81 (11)** (2007), p. 5429-5436.

[23] J. Lucchetti, M. Roy, M. Martcheva, An avian influenza model and its fit to human avian influenza cases", in *Advances in Disease Epidemiology* (J. M. Tchuenche, Z. Mukandavire, Eds.), Nova Science Publishers, New York, (2009), p. 1-30.

[24] J. Ma, Z. Ma, Epidemic threshold conditions for seasonally forced SEIR models, *Math. Biosci. Eng.* **3** (2006), p. 161-172.

[25] M. Marthceva, A Non-Autonomous Multi-Strain SIS Epidemic Model,*J. Biol. Dynamics*, Vol. 3 (2 &3), (2009), p. 235-251.

[26] , I.A. Moheim, Seasonally varying epidemics with and without latent period: a comparative simulation study, *Mathematical Medicine and Biology* **27** (2007), p. 1-15.

[27] E.J. Murray, S.S. Morse, Seasonal oscillation of human infection with influenza A/H5N1 in Egypt and Indonesia, *PLoS One* **6(9)** (2011): e24042.

[28] J. Nazir, R. Haumacher, A. Ike, P. Stumpf, R. Böhm, R.E. Marschang, Long-term study of avian influenza viruses in water (distilled water, normal saline, and surface water) at different temperatures, *Avian Dis.* **54** (2010), p. 720-724.

[29] R. Olinky, A. Huppert, L. Stone, Seasonal dynamics and thresholds governing recurrent epidemics, *J. Math. Biol.* **56** (2008), p. 827-839.

[30] B. Olsen, V.J. Munster, A. Wallensten, J. Waldenström, A.D M.E. Osterhaus, R.A.M. Fouchier, Global patterns of influenza A virus in wild birds, *Science* **312 (5772)** (2006), p. 384 - 388.

[31] A.W. Park, K. Glass, Dynamic patterns of avian and human influenza in east and southeast Asia, *Lancet Infect. Dis.* **7(8)** (2007), p. 543-548.

[32] J. S. M. Peiris, M. D. de Jong, Y. Guan, Avian influenza virus (H5N1): a threat to human health, *Clinical Microbiology Reviews*, (2007)p.243-267.

[33] J. M. Ponciano, M. A. Capistrán, First principles modeling of nonlinear incidence rates in seasonal epidemics, *PLoS Comput Biol* **7(2)** (2011): e1001079.

[34] J.B. du Prel, W. Puppe, B. Grondahl, M. Knuf, J.A. Weigl, *et al.*, Are meteorological parameters associated with acute respiratory tract infections? *Clin Infect Dis* **49** (2009), p. 861-868.

[35] D. J. Prosser, P. Cui, J. Y. Takekawa, M. Tan, *et. al.*, Wild Bird Migration across the Qinghai-Tibetan Plateau: A transmission route for Highly Pathogenic H5N1, *PLoS One* **6 (3)**, e17622.

[36] S.M. O'Regan, Impact of seasonality upon the dynamics of a novel pathogen in a seabird colony, *Journal of Physics: Conference Series* **138** (2008) 012017.

[37] B. Roche, C. Lebarbenchon, M. Gauthier-Clerc, C.M. Chang *et al*, Water-borne transmission drives avian influenza dynamics in wild birds: The case of the 2005-2006 epidemics in the Camargue area, *Inf. Gen. Evo.* **9** (2009), p. 800-805.

[38] P. Rohani, R. Breban, D.E. Stallknecht, J.M. Drake, Environmental transmission of low pathogenicity avian influenza and its implications for pathogen invasion, *PNAS* **106** (2009), p. 10365-10369.

[39] D.E. Stallknecht, S.M. Shane, M.T. Kearney, P.J. Zwank, Persistence of avian influenza virus in water, *Avian Dis.* **34** (1990), p. 406-411.

[40] D.E. Stallknecht, M.T. Kearney, S.M. Shane, P.J. Zwank, Effects of pH, temperature and salinity on persistence of avian influenza virus in water, *Avian Dis.* **34** (1990), p. 412-418.

[41] H. R. Thieme, Mathematics in Population Biology, Princeton University Press, (2003).

[42] W. Wang, X.-Q. Zhao, Threshold dynamics for compartmental epidemic models in periodic environments, *J. Dyn. Diff. Equat.* **20** (2008), p. 699-717.

[43] M.P. Ward, D. Maftei, C. Apostu, A. Suru, Estimation of the basic reproductive number (R0) for epidemic, highly pathogenic avian influenza subtype H5N1 spread, *Epidemiol Infect.* **137(2)** (2009) p. 219-226.

[44] T.P. Weber, N. I. Stilianakis, Migratory birds, the H5N1 influenza virus and the scientific method, *Virology Journal* **5:57** (2008) doi:10.1186/1743-422X-5-57.

[45] R.G. Webster, M. Yakhno, V.S. Hinshaw, W.R. Bean, K.G. Murti, Intestinal influenza; replication and characterization of influenza viruses in ducks, *Virology* **84** (1978), p. 268-278.

[46] J.P. Wood, Y.W. Choi, D.I. Chappie, J.V. Rogers, J.Z. Kaye, Environmental persistence of highly pathogenic avian influenza (H5N1) virus, *Environ. Sci. Technol.* **44 (19)** (2010), p. 7515-7520.
[47] U.S. Department of the Interior, USGS Field Manual of Wildlife Diseases General Field Procedures and Diseases of Birds, USGS, 1999.
[48] The Writing Committee of the WHO Consultation on Human Influenza A/H5, Avian influenza A (H5N1) infection in humans, *N. Engl. J. Med.* **353 (13)** (2005), p. 1374-1385.
[49] World Health Organization, Review of latest available evidence on potential transmission of avian influenza (H5N1) through water and sewage and ways to reduce the risk to human health, Geneva, 2006.
www.who.int/water_sanitation_health/.../h5n1background.pdf
[50] World Health Organization, Laboratory study of H5N1 viruses in domestic ducks: main findings, http://www.who.int/csr/disease/avian_influenza/labstudy_2004_10_29/en/
[51] Wikipedia, Life expectancy, http://en.wikipedia.org/wiki/Life_expectancy.
[52] World Health Organization, Confirmed Human Cases of Avian Influenza A(H5N1), http://www.who.int/influenza/human_animal_interface/H5N1_cumulative_table_archives/en/index.html

Department of Mathematics, University of Tulsa, Keplinger Hall - U337 800 S. Tucker Drive Tulsa, OK 74104-3189
E-mail address: necibe-tuncer@utulsa.edu

Department of Mathematics, University of Florida, 358 Little Hall, PO Box 118105, Gainesville, FL 32611–8105
E-mail address: maia@math.ufl.edu